LIMNOLOGY and OCEANOGRAPHY

ASLO

Limnol. Oceanogr. 9999, 2024, 1–14

doi: 10.1002/lno.12757

Bloom compression alongside marine heatwaves contemporary with the Oregon upwelling season

Ian T. Black ,* **Maria T. Kavanaugh** , **Clare E. Reimers**
College of Earth, Ocean, and Atmospheric Sciences, Oregon State University, Corvallis, Oregon, USA

Abstract

Marine heatwave (MHW) events have led to acute decreases in primary production and phytoplankton biomass in the surface ocean, particularly at the mid latitudes. In the Northeast Pacific, these anomalous events have occasionally encroached onto the Oregon shelf during the ecologically important summer upwelling season. Increased temperatures reduce the density of offshore waters, and as a MHW is present offshore, coincident downwelling or relaxation may transport warmer waters inshore. As an event persists, new upwelling-driven blooms may be prevented from extending further offshore. This work focuses on MHWs and coincident events that occurred off Oregon during the summers of 2015–2023. In late summer 2015 and 2019, both documented MHW years, coastal phytoplankton biomass extended on average 6 and 9 km offshore of the shelf break along the Newport Hydrographic Line, respectively. During years not influenced by anomalous warming, coastal biomass extended over 34 km offshore of the shelf break. Reduced biomass also occurs with reduced upwelling transport and nutrient flux during these anomalous warm periods. However, the enhanced front associated with a MHW aids in the compression of phytoplankton closer to shore. Over shorter events, heatwaves propagating far inshore also coincide with reduced chlorophyll *a* and sea-surface density at select cross-shelf locations, further supporting a physical displacement mechanism. Paired with the physiological impacts on communities, heatwave-reinforced physical confinement of blooms over the inner-shelf may have a measurable effect on the gravitational flux and alongshore transport of particulate organic carbon.

Described as prolonged yet anomalous increases in sea-surface temperature (SST), marine heatwaves (MHWs) are anticipated to escalate in frequency and duration globally with anthropogenic warming (Frölicher et al. 2018; Oliver et al. 2018). At high latitudes, phytoplankton biomass has been observed to increase during surface MHWs (Batten et al. 2022; Noh et al. 2022). Conversely, at the mid and lower latitudes, reduced phytoplankton biomass in the surface ocean, both during and following a MHW, has been a common observation among biogeochemical studies of the phenomenon (Sen Gupta et al. 2020; Suryan et al. 2021; Noh et al. 2022). Thermally induced physiological stress (Baker and Geider 2021; Samuels et al. 2021; Smith et al. 2023) and shoaling of the surface mixed layer paired with reduced macronutrient input (Hayashida et al. 2020) have been hypothesized as key modes that reduce surface biomass during periods of anomalous warming. As MHWs continue to intensify, the severity of phytoplankton biomass reduction is expected to increase (Hayashida et al. 2020) along with shifts in community structure (Remy et al. 2017). Santora et al. (2020) previously suggested that MHWs compress cooler upwelling system habitat toward nearshore environments and highlighted associated changes in forage species and whale distributions through ecosystem surveys. Many studies to date have emphasized the global and regional impacts that MHWs have on phytoplankton biomass (Noh et al. 2022) and other trophic levels (Smith et al. 2023); however, finer-scale biophysical studies documenting changes in phytoplankton distributions are less common.

Within the last decade in the Northeast Pacific, two MHWs have become notorious for their ecological and socioeconomic impacts (Smale et al. 2019; Wyatt et al. 2022). The "Blob" first

*Correspondence: blackia@oregonstate.edu

Additional Supporting Information may be found in the online version of this article.

Author Contribution Statement: IB: Conceptualization; Data Curation; Formal Analysis; Investigation; Methodology; Software; Validation; Visualization; Writing – original draft preparation; Writing – review and editing. MTK: Supervision; Writing – review and editing. CER: Funding acquisition; Project administration; Supervision; Writing – review and editing.

Special Issue: Autonomous Instrumentation and Big Data: New Windows, Knowledge, and Breakthroughs in the Aquatic Sciences. *Edited by: Yui Takeshita, Heidi Sosik, Dominique Lefevre, Werner Eckert, Kevin C. Rose and Deputy Editors Julia C. Mullarney, Steeve Comeau, and Elisa Schaum.*

appeared in winter 2013 within the Gulf of Alaska and held fast in the Northeast Pacific well through 2016, becoming of interest for its multiyear residence, particularly between 2014 and 2015. The heatwave's enhanced SSTs developed with reduced air–sea heat flux and reduced surface mixing, which was driven from strong and chronic weather patterns associated with high sea-level pressure (Bond et al. 2015). The "Blob 2.0" appeared in the southern portion of the Gulf of Alaska in Spring/Summer 2019, where it approached the Oregon coast toward the middle of the upwelling season and persisted until late 2019. Although comparatively short lived to the 2014–2015 MHW, the 2019 MHW was of interest for its strong intensity, proximity to the West coast of the United States, and seasonally opposite initiation. It was driven by a weakening of the North Pacific High, which resulted in a series of consequences similar to the 2014–2015 MHW, such as reduced surface winds and wind-driven upper ocean mixing. Surface heat fluxes then transferred to a thinner surface mixed layer, which created and retained anomalously warm sea surface temperatures (Amaya et al. 2020). Marine heatwaves sharing similar characteristics have been identified in the greater Northeast Pacific as far back as 1983 using strength (> 1.29 time the standard deviation of the SST anomaly integrated over the MHW area) and spatial extent (> 400,000 km^2) as key identifiers (Leising et al. 2024).

Upwelling has been described as having a buffering effect against MHWs in eastern boundary upwelling systems (Peterson et al. 2016; Varela et al. 2021), such as the Northern California Current System. In this region, periods of sustained equatorward wind stress result in offshore Ekman transport (Kudela et al. 2008; Kämpf and Chapman 2016), prominently during the spring and summer months. As surface water is transported offshore, deeper water must be brought to the surface to satisfy continuity. This upwelled water is generally cooler, more saline, and more nutrient-rich than the displaced surface waters and is an important driver of marine ecosystem productivity (Barth et al. 2019). Conceptually, if a MHW water mass develops over the shelf, those waters will be displaced offshore with movement of the surface Ekman layer during periods of strong upwelling, but the opposite must also hold true when upwelling is weak, relaxed, or there is a shift to downwelling conditions. In this work, the primary focus is the central Oregon shelf, where seasonal upwelling is intermittent through the months of May–October, interspersed with episodes of relaxation and downwelling (Checkley and Barth 2009; Kämpf and Chapman 2016). Further south (south of Cape Blanco), upwelling is more persistent in select areas, much like the rest of the Southern California Current System (Checkley and Barth 2009).

The atmospheric drivers of MHWs are not discussed in detail in this work, only their complementary impact on surface winds and transport associated with wind-driven upwelling. A reduction in upwelling associated with a regional atmospheric MHW driver, as well as an enhanced front at the intersection of MHW waters and nearshore water masses may influence not only the total phytoplankton biomass in the coastal ocean, but also its spatial distribution and export. Under typical, non-MHW conditions, the gravitational flux of phytoplankton and subduction of particulate organic matter may occur most intensely at the intersection of mesoscale fronts (Stukel et al. 2017, 2018; Boyd et al. 2019) and seaward of the shelf. Marine heatwaves and their drivers may promote physical conditions that enhance frontal gradients and retain phytoplankton distributions and export more landward. Coastal shelves are estimated to receive as much as 48% of the global seafloor carbon flux (Dunne et al. 2007), thus particularly intense and prolonged upwelling-contemporary MHW periods may increase the food supply to benthic communities and impact carbon sequestration occurring on shelves while reducing offshore export. The initial challenge in documenting this assertion is identifying a relationship between nearshore MHWs, the MHW driver impact on upwelling, and phytoplankton biomass compression.

Our basic hypothesis rests on the well-known process of frontogenesis occurring between offshore and recently upwelled waters. Under typical conditions, a density gradient occurs between these waters, but during MHW periods, the density gradient at this front is enhanced. As a MHW feature from offshore persists over the shelf or is accelerated inshore due to relaxation/downwelling conditions, this would then effectively confine nutrient delivery and responding chlorophyll *a* (Chl *a*) signals to locations closer to shore. Continued presence of a MHW during weak upwelling would also have a similar effect. Under non-MHW conditions, it is then presumed that surface Chl *a* signals extend further offshore, potentially reaching over the continental slope and abyssal plain. To test this hypothesis, the spatial patterns of Chl *a* during the Oregon upwelling season in years 2015–2023 are investigated using a combination of coastal indices, satellite ocean color images, moored biogeochemical sensors, and blended data products.

Methods

Region of interest and data access

Our region of interest is the Oregon shelf with attention given to observations made in the vicinity of the Newport Hydrographic (NH) Line (Fig. 1). This area is actively sampled by in-situ observational programs such as the National Science Foundation's Ocean Observatories Initiative (OOI) Endurance Array, which maintains three cross-shelf sites off Oregon that have been instrumented since 2015 (Table 1, Fig. 1) (OOI 2022). The NH Line has also been monitored in campaign-style studies by a number of research institutions and NOAA for many decades, leading to the creation of open-access datasets and established surface water climatologies (Risien et al. 2022, 2023). Flyovers from National Aeronautics and Space Administration (NASA) and National Oceanic and Atmospheric Administration (NOAA) satellites provide adequate coverage for the creation of daily common grid datasets.

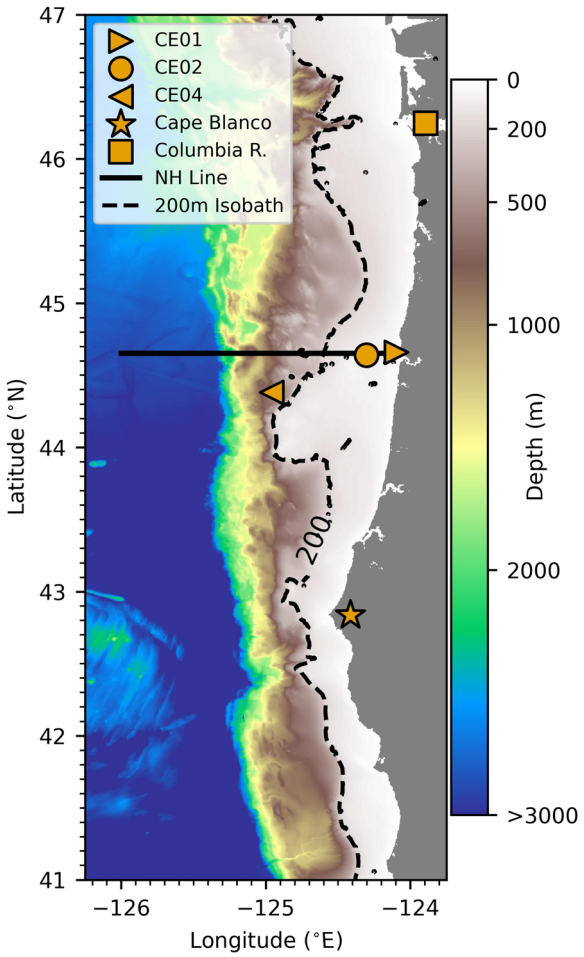

Fig. 1. A bathymetric map of the study region off the Oregon coast. A black dashed contour marks the 200 m isobath, considered in this study to represent the shelf break. The locations of the Ocean Observatories Initiative (OOI) Endurance Array Oregon sites, Cape Blanco, and the mouth of the Columbia River are marked for reference. Bathymetry data are General Bathymetric Chart of the Oceans 2023 (International Hydrographic Organization 2024).

No data were collected experimentally, and only open-access data were used in this research. Analysis was performed and additional data products were computed using the base parameters of sea water temperature, practical salinity, water pressure, fluorometric and satellite-derived Chl *a*, the Coastal Upwelling Transport Index (CUTI), and the Biologically Effective Upwelling Transport Index (BEUTI) (Jacox et al. 2018). Details regarding data access methods and intermediate processing steps can be found in the project repository README and the code modules that accompany this research (https://github.com/IanTBlack/oregon-shelf-mhw).

OOI mooring time series

In this work, each Oregon site of the OOI Endurance Array (https://oceanobservatories.org/array/coastal-endurance/) is referenced by its simplified OOI site identifier (Table 1). CE01 and CE02 lie roughly along the NH Line, with the CE02 site effectively taking over the role of the legacy NH10 mooring at the mid-point of the Oregon shelf (Fig. 1). CE04 is south of the NH Line and is located seaward of the shelf break on the slope. Each OOI site hosts a surface mooring with a variety of physical and biochemical sensors at 1 and 7 m depth, a seafloor sampling package, and a profiler that spans the majority of the water column. Links are provided in the project repository README that further describe the specific platforms and sensors at each site.

All methods of data collection performed by the OOI were combined (e.g., telemetered data and data recovered from sensor memory), and duplicate sample records were dropped to produce the most complete record possible. Data were excluded if the Integrated Ocean Observing System quality assessment primary flag was either bad (flag = 4) or missing (flag = 9) (OOI 2023). The custom quality control test results produced by the OOI were not utilized in quality assessment because there has been indication that the OOI will move away from these tests in favor of the Integrated Ocean Observing System variants in the future (Palevsky et al. 2023).

All time series were binned into daily averaged values and filtered with a centered 11-d running mean for visualization. Temperature, practical salinity, and pressure were acquired from sensors located at 7 m depth on the mooring at each of the three sites. Time series of conservative temperature, absolute salinity, and density were then calculated at each respective site using the Gibbs-Seawater package (Barna et al. 2024). Fluorescence-based Chl *a* concentration records were also collected from sensors located at 7 m depth on the moorings, and a rough mean climate time series, based on 8 yr of OOI data, was derived to aid in the identification of key bloom periods at each site. No additional corrections, validations, or comparisons were performed on OOI Chl *a* data.

Table 1. Ocean Observatories Initiative (OOI) Endurance Array Oregon Sites. Additional information about the OOI Coastal Endurance Array and the sampling platforms in use can be found in the project repository README or on the OOI website: https://oceanobservatories.org/array/coastal-endurance/

Site ID	Name	Location	Offshore distance (km)	Water depth (m)
CE01	Oregon Inshore	44.6598°N, −124.095°E	3	25
CE02	Oregon Shelf	44.6393°N, −124.304°E	20	80
CE04	Oregon Offshore	44.3811°N, −124.956°E	68	588

Identifying upwelling season coincident warming events

Prior derivations of the spring and fall transition dates through the Columbia Basin Research Mean method (https://www.cbr.washington.edu/dart/trans, Holmes 2007) were used to define the upwelling season for each year. The CUTI and BEUTI model products (Jacox et al. 2018; Jacox 2024) were used to compare upwelling records between years. These datasets can be obtained as daily values which indicate total vertical transport through the base of surface mixed layer in 1° latitude bins. CUTI specifically focuses on the vertical transport of water, while BEUTI focuses on vertical nitrate flux with respect to the surface mixed layer.

The NOAA Optimum Interpolation SST V2 dataset provides daily mean SST with global coverage on common 0.25° grid cells by combining observations from satellites and in situ sources (NOAA 2023). Files were collected for the years 1983–2023 for the region of interest (41 yr). A mean and 90th percentile climatology were then calculated with a centered 11-d running mean for each cell in the region to facilitate MHW identification and categorization following an established MHW classification framework (Hobday et al. 2016, 2018). A key difference is that a 41-yr climatology baseline was used in this work, which also included the years that underwent analysis, instead of the recommended 30-yr period (Hobday et al. 2016). Anomalously warm periods are initially referred to as warming events in the results and MHW status is later attributed in the discussion. Events were only utilized in analysis if they occurred within or overlapped with a year's upwelling season.

Upwelled waters that are transported over the shelf and out to CE04 may intercept persistent and intense MHWs, creating conditions that appear as shorter discrete warming events. Such interceptions are more likely to occur farther inshore where isopycnals first rise to the surface. Years other than 2015 and 2019 are not prominently featured in the literature as having intense or prolonged MHWs close to shore, but tools such as the California Current Marine Heatwave Tracker (Blobtracker) describe the occurrence of spatially large MHWs in the greater Northeast Pacific between 2015 and 2023 (Leising et al. 2024). To help identify the source of any discrete MHWs that were identified at CE04, Blobtracker data were used to confirm if study-identified MHWs were also contemporary with a MHW within the greater Northeast Pacific. Marine heatwaves occurring in rapid succession were then assumed to be coupled events, originating from an offshore MHW and discretized by upwelling rather than as an event with unique origins. The caveats of using these delimiters can are further described in the discussion section.

Analysis period of interest

Through the described MHW identification methods in conjunction with prior literature, it was identified that the 2019 MHW was frequently present at CE04 between July 9 and October 8 in 2019. Intense but shorter events were also identified during the same analysis period in 2023. For other years, including 2015, anomalously warm events at CE04 were not as prominent over this time span. This time period is also of interest due to its co-occurrence with the warmest time of year for surface waters near CE04 and the timing of the summer bloom regionally (Venegas et al. 2008). In creating composite images and performing interannual comparisons of time series, we focused on data spanning the 92 d between July 9 and October 8 for each year.

Identifying upwelling-influenced biomass

NASA's Moderate Resolution Imaging Spectroradiometer-Aqua Ocean Color Level 2 dataset provides satellite-derived Chl *a* in asymmetric swath files (NASA 2022). Files were collected for each day between July 9 and October 8 (92 d), 2015–2023. Chl *a* values that were flagged as fail (flag = CHLFAIL, ATMFAIL, or NAVFAIL) were excluded from analysis along with values flagged as suspect (flag = CHLWARN). Pixels outside the range of 0–35 $\mu g\ L^{-1}$ were also excluded from analysis (Kavanaugh et al. 2015). Swaths were linearly interpolated to 0.01° grid cells and overlapping daily swaths were averaged to create a single-day grid file. We were only able to create 89 grid files for 2020 due to processing issues and 85 files for 2023 due to lack of data availability between October 2 and October 8. Composites of periods of interest were created by averaging daily files and were used in interannual comparisons.

Although it is a poor proxy in oligotrophic oceans (Behrenfeld et al. 2005), Chl *a* derived from both satellite and in situ sensor measurements has been historically used to infer phytoplankton biomass (Huot et al. 2007; Blondeau-Patissier et al. 2014; Noh et al. 2022). Offshore of the Oregon shelf, Chl *a* ranges on average between 0.25 and 0.5 $\mu g\ L^{-1}$ (Sarmiento and Gruber 2006), with maxima reaching upward of 0.78 $\mu g\ L^{-1}$ (Tweddle et al. 2010). A static threshold of 0.75 $\mu g\ L^{-1}$ was used to delineate upwelling-driven coastal biomass from background open ocean signals when evaluating both satellite and OOI sensor–derived Chl *a*. The guiding assumption is that offshore MHW waters are distinct in their Chl *a* concentrations and density when compared to nearshore water masses. A threshold of 2.3 $\mu g\ L^{-1}$ was also used to infer concentrated and primarily upwelling-fed biomass (determined using the 90th percentile of CE04 Chl *a* data from years 2015 to 2023 as the discriminator). A similar off-shelf band maximum of 2.5 $\mu g\ L^{-1}$ was also identified by Venegas et al. (2008). Daily averaged composites were then created with data between July 9 and October 8 for each year. Coastal Chl *a* isopleths in figures were denoised with a Gaussian filter to assist in visualization. Along the NH Line, the locations of the values closest to each threshold were used to compute cross-shelf distance in reference to the shelf break (−124.6°E).

Results

Warm events

Nineteen events meeting the criteria of a MHW were identified at CE04 during the upwelling seasons of 2015–2023

(Table 2; Fig. 2) using NOAA Optimum Interpolation SST V2 data. No warming events were identified for the seasons of 2017, 2020, and 2021. The site experienced severe, strong, and several moderate events which persisted for most of the first half of the upwelling seasons of 2015 and 2016. In 2018, warm events occurred in the first half of the upwelling season but were only classified as moderate and were relatively brief in duration (5–7 d). Year 2018 is also unique in that no parent MHWs were identified in the greater Northeast Pacific in Blobtracker data. In 2019, the site experienced the most intense event of those identified ($i_{max} = 4.5°C$) for a period of 40 d (Table 2). Events identified during the 2019 upwelling season were also more intense on average compared to other years. The average intensity of the two warm events in 2023 was comparable to 2019, although shorter in duration.

As stated previously, we concentrated our data synthesis between July 9 and October 8 for each year, which encompasses the warmest time of the year at CE04 and when warm events occurred in rapid succession in summer 2019 (marked in bold in Table 2). Regional SST coverage showed anomalously warm temperatures between July 9 and October 8 offshore (< −125°E) of the Oregon shelf for all years (Fig. 3). Corroborated by the time-series analysis results for CE04 (Fig. 4), warm temperatures were not largely present along the majority of the Oregon shelf in 2017 and 2021 (with only some minor presence east and south of Cape Blanco). However, in 2020, potential MHW signals appeared along the shelf north and south of the NH Line for roughly 30% of the analysis period. In 2015, warm anomaly presence along the NH Line was short, but to the north and south, warm days were present about 60% of the time. In 2016, warm signals were only present at the furthest outreach of the NH Line. In 2019, signals were present 60–80% of the time north of Cape Blanco, with presence reaching 100% just south of CE04 near Heceta Bank, indicating the largest temporal and spatial anomalous warming coverage for the analysis period across all years. At the upwelling loci near Newport, OR and south of Cape Blanco, potential MHW presence was much less (∼ 20–30%) in 2019. In 2022, anomalous warming was mostly identified north and south of the NH Line and off the shelf for 20–60% of the analysis period. In 2023, warm waters were more prominent offshore of CE04 and the northern coast of Oregon, but rarely occurred along the shelf south of the Columbia River.

Upwelling, temperature, salinity, and density

Warm events coincided with downwelling, upwelling, or a combination of both (Fig. 4). For events with a short duration, initiation tracked with downwelling or a trend to relaxation. Termination of short events also coincided with a shift to upwelling or a period of relaxation that was then followed by subsequent upwelling. Events with a longer

Table 2. Upwelling season warm events detected near CE04. T_s and T_e are the start and end dates of an identified event. D is the duration of the event in days. i_{max}, i_{mean}, and i_{var} are the intensity maximum, mean, and variance in °C (Hobday et al. 2016). Category is the peak category over the course of the event (Hobday et al. 2018). Blob ID is the feature ID of a contemporary MHW identified through the Blobtracker dataset (Leising et al. 2024).

T_s	T_e	D (days)	i_{max} (°C)	i_{mean} (°C)	i_{var} (°C)	Peak category	Blob ID
2014-11-27	2015-04-21	146	2.87	2.04	0.48	Severe	NEP2013d
2015-04-24	2015-05-01	8	1.70	1.13	0.38	Strong	NEP2013d
2015-07-23	2015-07-28	6	2.69	2.40	0.24	Moderate	NEP2013d
2015-10-20	2015-10-24	5	1.58	1.42	0.16	Moderate	NEP2013d
2016-03-29	2016-04-12	15	2.12	1.68	0.29	Strong	NEP2016a
2016-04-17	2016-05-05	18	2.47	1.79	0.41	Severe	NEP2016a
2016-05-22	2016-05-26	5	1.82	1.72	0.13	Moderate	NEP2016a
2016-05-29	2016-06-06	9	2.21	1.73	0.32	Moderate	NEP2016a
2018-05-15	2018-05-21	7	1.73	1.62	0.15	Moderate	None
2018-06-06	2018-06-12	7	1.94	1.67	0.20	Moderate	None
2018-06-20	2018-06-25	6	2.19	1.81	0.26	Moderate	None
2018-07-07	2018-07-11	5	2.16	1.97	0.16	Moderate	None
2019-07-09	2019-07-19	11	3.12	2.61	0.28	Moderate	NEP2019c
2019-07-23	2019-07-28	6	2.52	2.32	0.19	Moderate	NEP2019c
2019-08-07	2019-08-16	10	3.25	2.90	0.34	Moderate	NEP2019c
2019-08-30	**2019-10-08**	40	4.50	2.77	1.05	Severe	NEP2019c
2022-07-07	2022-07-11	5	2.55	2.20	0.31	Moderate	NEP2022a
2023-08-08	2023-08-12	5	3.04	2.67	0.34	Moderate	NEP2023a
2023-08-27	2023-09-02	7	2.95	2.62	0.23	Moderate	NEP2023a

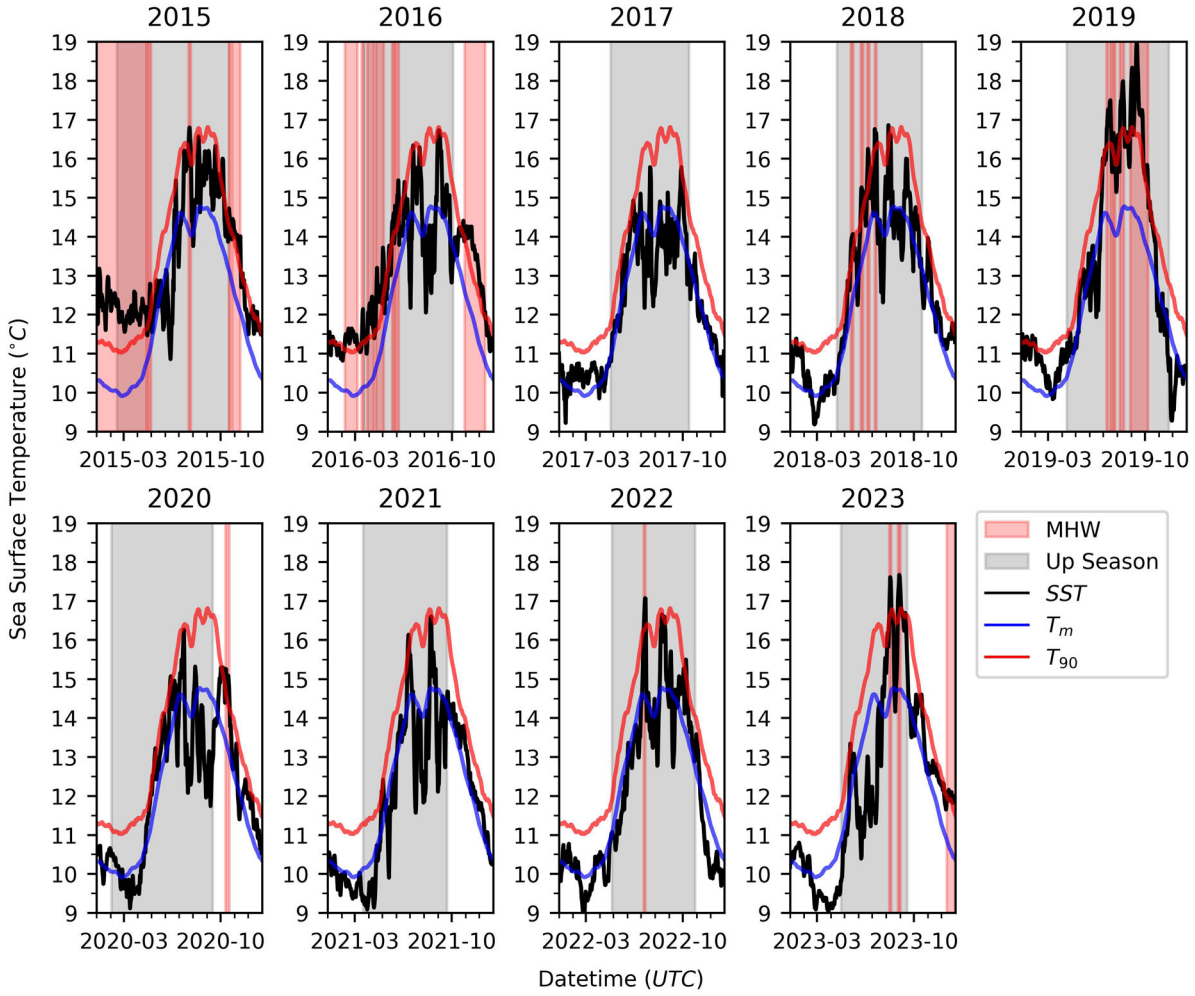

Fig. 2. Sea-surface temperature (SST) records highlighting warm events observed at CE04. This figure includes events (red vertical spans) identified both during and outside of each year's upwelling season (gray vertical spans). Potential marine heatwave (MHW) events were identified from NOAA Optimum Interpolation daily mean SST data for a cell near CE04 using methods described by Hobday et al. (2016). Periods exceeding the 90th percentile for a length of 5 or more days were classified as potential MHW events. T_m (blue) is the climatological mean at that cell computed with a centered 11-d rolling window. T_{90} (red) is the historic 90th percentile for each day based on 41 yr of data, also computed with an 11-d rolling mean. Black indicates daily mean SST.

duration (e.g., Table 2: 2016-04-17; 2019-08-30) were observed to occur alongside sustained and weak upwelling, with only a few days of downwelling throughout the event. Average upwelling during known MHW years (2015, 2019) was at minimum 30% weaker than upwelling during non-MHW years (2017, 2020, 2021).

Upwelling season warm events identified at CE04 using regional SST aligned with local peaks in the conservative temperature time series computed from the CTD located at 7 m depth on the CE04 mooring (Fig. 4). Salinity was typically near or above 32 ASU during individual events. However, some warm events that occurred in 2016, 2018, and 2022 coincided with drastic decreases in salinity down to 31 ASU and sometimes below 30 ASU. Seawater density during warm events was typically between 1023 and 1024 kg m^{-3}. Similar in trend to salinity for 2016, 2018, and 2022, density dropped below 1022 kg m^{-3} for some events, suggesting salinity contributed much more to density in these instances. From data averaged between July 9 and October 8, the CE04 site in 2019 had the greatest daily water temperature, lowest density, lowest Chl *a*, and lowest nitrate flux (Table 3).

Chlorophyll *a* and nitrate flux

At CE04, individual warm events aligned with periods where Chl *a* was much lower than the time-series average (1.4 μg L^{-1}) and the climatological mean (Fig. 4, using 2015–2023 data). The analysis period for 2019 had the lowest average Chl *a* and daily averaged modeled nitrate flux across all years (Table 3). For years that did not have substantial MHW presence during the analysis period at CE04 (2016, 2017,

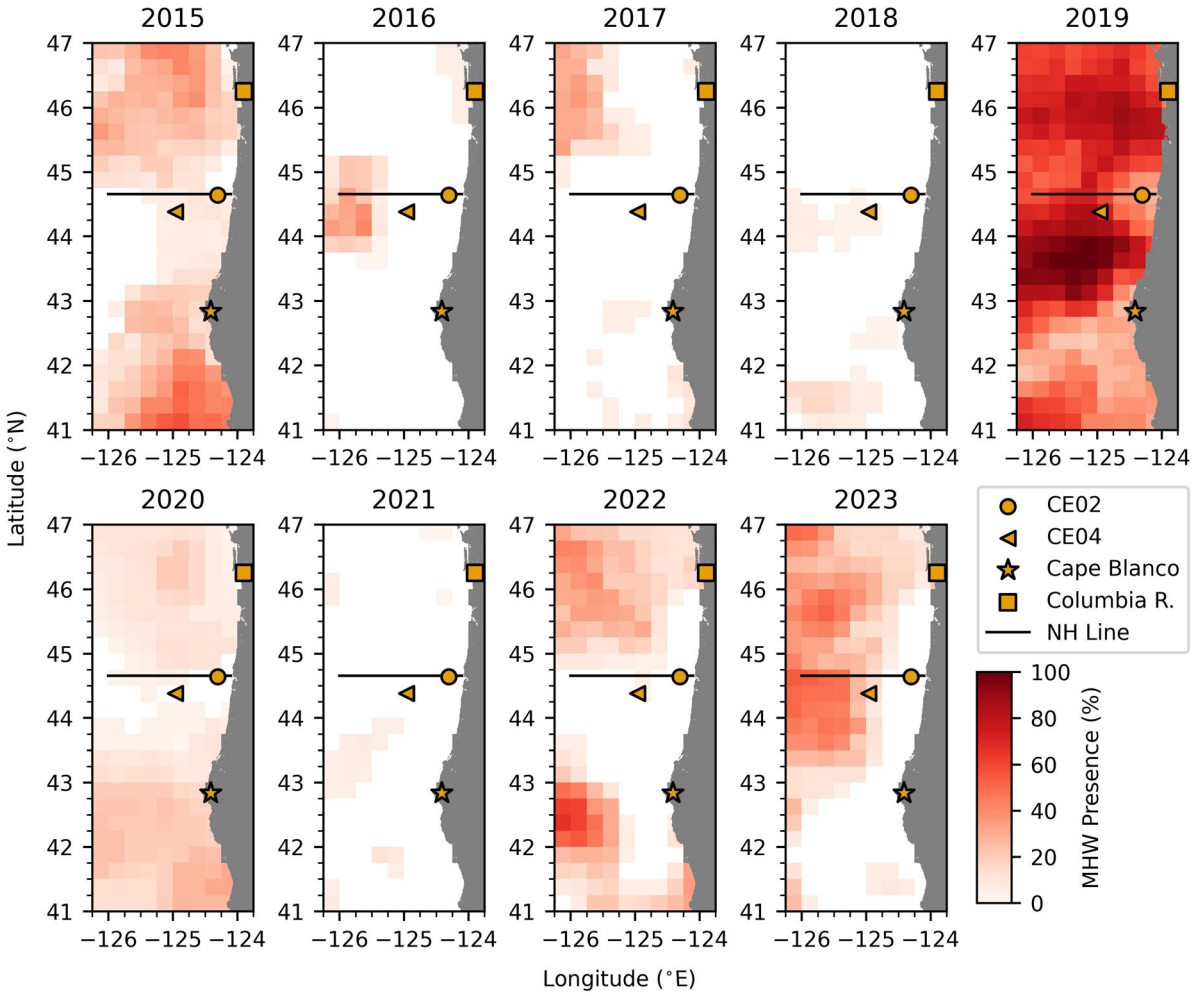

Fig. 3. Composites of marine heatwave (MHW) presence between July 9 and October 8 for 2015–2023. Each cell value represents the percentage of MHW days that occurred in that cell between the target dates (92 d). For example, if a cell displays a value of 60%, then 60% of the days between July 9 and October 8 (or 55 d) were classified as MHW days.

2018, 2020, 2021, and 2022), the nitrate flux was 40–75% greater than known MHW years (2015, 2019). Similar to CE04, most of the upwelling season warm events identified at CE02 and CE01 were also contemporary with reduction in Chl *a* (Supporting Information Figs. S1, S2).

From the CE04-derived Chl *a* climatology, we observed an occurrence of a regular spring bloom (April) and a summer bloom (September). The peak of the summer bloom appears contemporary with the warmest time of year at CE04, and years 2019 and 2023 were the only years that experienced MHWs during this same period. The summer blooms of 2019 and 2023 at CE04 were also noticeably suppressed and difficult to differentiate from surrounding Chl *a* values (Fig. 4).

In Fig. 5, the offshore end of the NH Line in 2017, 2018, 2020, 2021, and 2022 all had greater Chl *a* values compared to years with anomalous warming (2015, 2016, 2019, and more recently 2023). The point at which we observe the transition from open ocean to upwelling-influenced biomass during normal years occurs much further offshore compared to the warmer years (Fig. 6). With respect to the shelf break along the NH Line, the open-ocean threshold (0.75 μg L^{-1}) occurred 6 and 9 km offshore of the shelf break (−124.6°E) for 2015 and 2019, respectively (Table 4). During other years, this delimiter was more than 30 km offshore. Reviewing the concentrated biomass threshold (2.3 μg L^{-1}), we observe that higher concentrations were confined, on average, 25 and 18 km inshore of the shelf break for 2015 and 2019. For other years, blooms on average either reached offshore of the shelf break or within 9 km inshore of the shelf break, an approximate minimum difference of 9 km between MHW and non-MHW periods. Between the analysis periods for each year, there was no drastic difference observed in the average amount of Chl *a* at CE01 along the NH Line (Fig. 6). However, individual MHW events

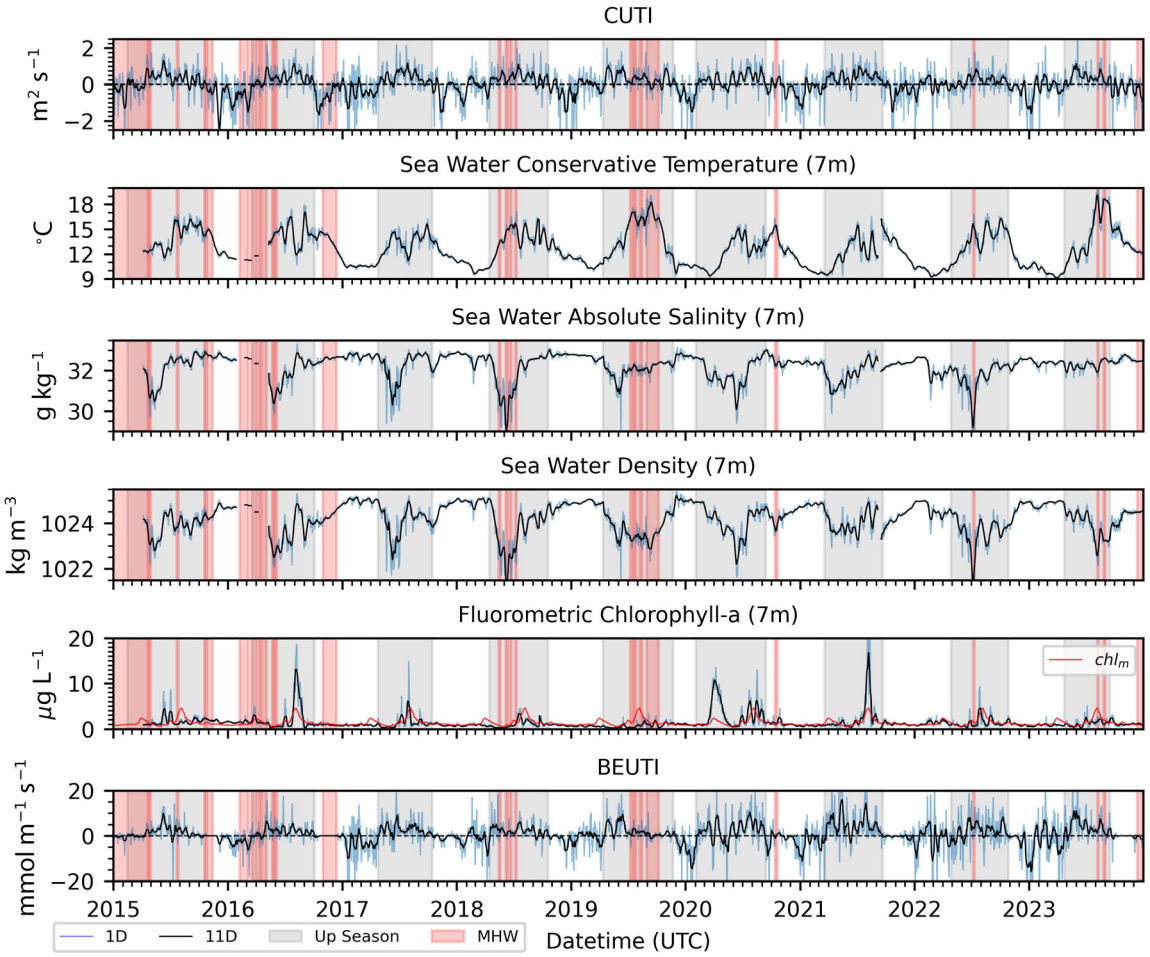

Fig. 4. Ocean Observatories Initiative (OOI) CE04, Coastal Upwelling Transport Index (CUTI), and Biologically Effective Upwelling Transport Index (BEUTI) time series between 2015 and 2023. Daily mean values are in light blue. Red vertical spans indicate potential marine heatwave (MHW) events and gray vertical spans indicate the time between the spring and fall transition dates. A centered 11-d rolling mean was applied to smooth the data (black).

Table 3. Daily averages at CE04 between July 9 and October 8. Conservative temperature, absolute salinity, density, and chlorohyll a (Chl *a*) were derived from sensors located at 7 m depth. Coastal Upwelling Transport Index (CUTI) and Biologically Effective Upwelling Transport Index (BEUTI) represent values modeled at the base of the surface mixed layer (Jacox et al. 2018; Jacox 2024).

Year	Conservative temperature (°C)	Absolute salinity (ASU, g kg^{-1})	Density (kg m^{-3})	Chl *a* (μg L^{-1})	CUTI (m^2 s^{-1})	BEUTI (mmol m^{-1} s^{-1})
2015	15.33	32.56	1023.94	1.50	0.259	1.04
2016	14.43	32.26	1023.90	3.42	0.385	1.83
2017	13.57	32.62	1024.35	1.95	0.446	2.40
2018	14.30	32.33	1023.98	1.61	0.374	2.12
2019	16.60	32.12	1023.33	0.87	0.214	0.98
2020	13.20	32.52	1024.35	2.87	0.346	2.75
2021	13.28	32.32	1024.17	4.54	0.423	4.05
2022	14.48	31.75	1023.50	1.66	0.295	2.82
2023	16.38	32.36	1023.55	1.56	0.197	1.96

occurring far inshore are contemporary with reduced Chl *a* and sea-surface density (Fig. 4; Supporting Information Figs. S1, S2), suggesting a finer-scale biophysical effect.

Away from the NH Line, a secondary observation was that biomass expansion between years was not consistent (Fig. 5). Where there was a high number of MHW days in Fig. 3, the

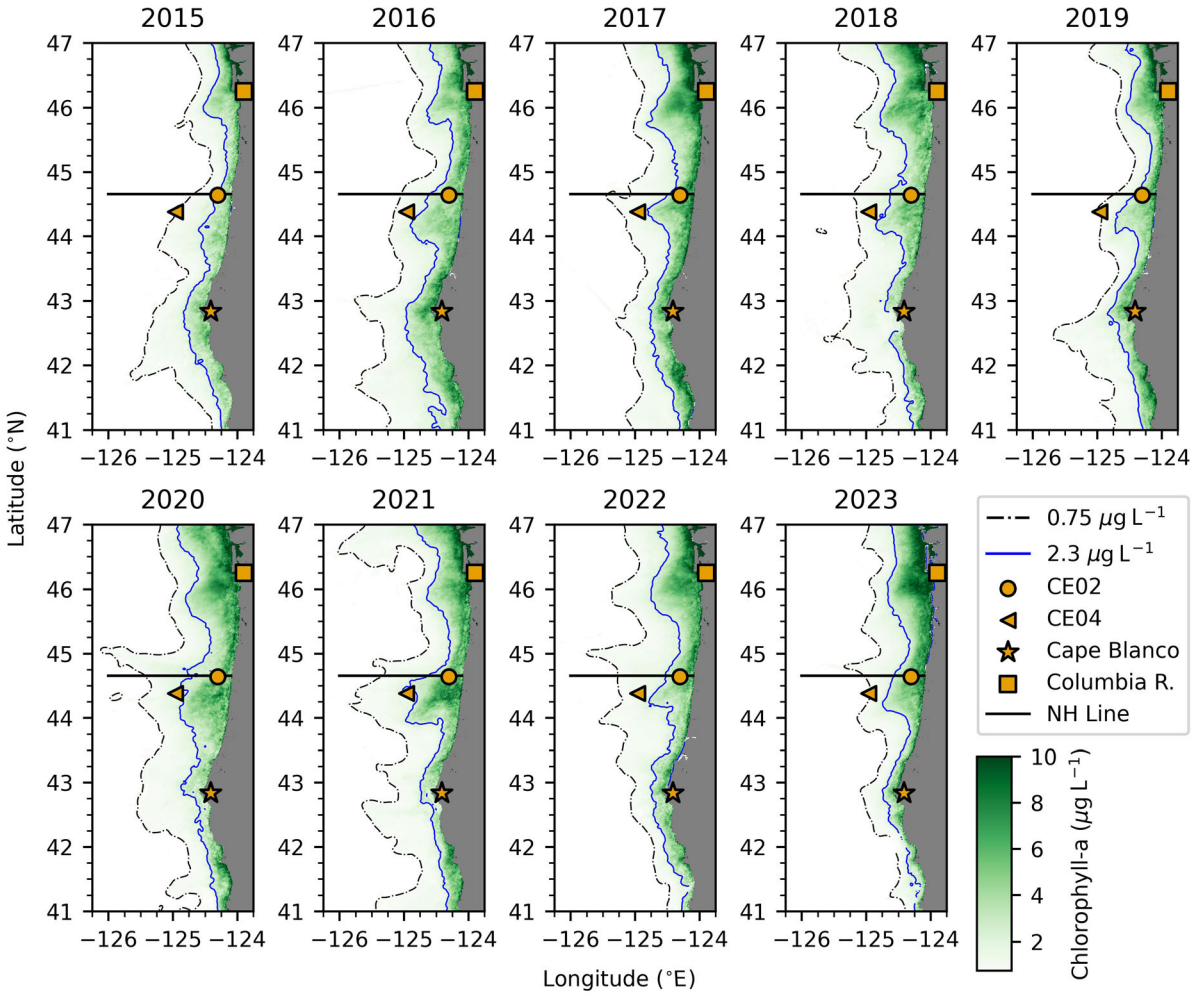

Fig. 5. Composites of average daily chlorophyll a (Chl *a)* between July 9 and October 8 for each year. A Gaussian filter ($\sigma = 4.5$ for 0. 75 μg L^{-1}, $\sigma = 1.5$ for 2.3 μg L^{-1}) was applied to smooth data for visualization. The black dash-dot contour represents the open-ocean Chl *a* threshold (0. 75 μg L^{-1}) and the blue solid contour indicates the threshold used to aid in the quantification of compression of upwelling-driven biomass 2.3 μg L^{-1}).

offshore position of each isopleth was restricted. During years not containing MHW days within the area, cross-shelf extent was much further in the north. Cross-shelf extent at and south of Cape Blanco appeared to be less connected to MHW presence in space and time.

Discussion

Marine heatwaves along the Oregon coast

The discrete warming events identified just offshore of CE04 in 2015, 2019, 2022, and 2023 appear to have been extensions from parent MHWs within the greater Northeast Pacific. The MHW presence results (Fig. 3) suggest that the impact of the 2014–2015 MHW was much more pronounced to the north and south of the NH Line during the late summer. This could be potentially explained by the splitting of the MHW by local upwelling-favorable winds identified by Fewings and Brown (2019).

Paired with reduced upwelling and nitrate flux to the surface, prior MHW presence likely explains the reduced offshore position of the Chl *a* isopleths in 2015. With the 2014–2015 MHW's long residence and its driver's suppression effect on upwelling (Amaya et al. 2016), by the summer of 2015 alongshore and transported phytoplankton biomass was already reduced in the region, which may explain the isopleth placement along the NH Line despite infrequent MHW detection at CE04 between July 9 and October 8.

El Niño is a climatic driver that can produce conditions that can be classified as or enhance existing MHWs (Sen Gupta et al. 2020). According to the Multivariate El Niño-Southern Oscillation Index (https://psl.noaa.gov/enso/mei/), the years 2015, 2018, and 2023 all hosted strong positive indices indicating that El Niño was likely a primary contributor to

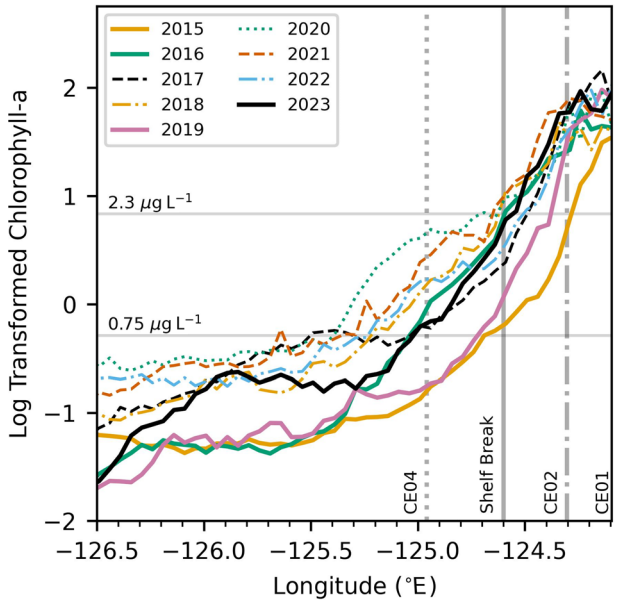

Fig. 6. Cross-shelf gradients of chlorophyll *a* (Chl *a*) along the Newport Hydrographic (NH) Line. Data are the daily average values between July 9 and October 8 for each year. The shelf break along the NH Line is located at −124.6°E.

Table 4. Estimated isopleth distances with respect to the shelf break along Newport Hydrographic (NH) Line. Distances are calculated as geodesic distance in kilometers. Positive values (+) indicate distance (km) offshore of the shelf break (seaward). Negative (−) values indicate distance inshore of the shelf break (landward).

Year	0.75 μg L^{-1}	2.3 μg L^{-1}
2015	+6	−25
2016	+35	+1
2017	+35	−9
2018	+49	+2
2019	+9	−18
2020	+63	+2
2021	+57	+4
2022	+51	−6
2023	+34	−3

warm sea surface temperature anomalies in the region during those years. For 2017, 2020, 2021, and 2022, indices were strongly negative. Year 2016 was unique in that positive indices were observed early in the year and then transitioned to weakly negative between July and October. Year 2019 was unique because the positive state of the El Niño-Southern Oscillation was weak (or near neutral) during the analysis period, suggesting that El Niño very weakly contributed to the warm surface anomalies observed during the 2019 summer.

Along the Oregon coast, reduced upwelling in the summer can be associated with El Niño (Corwith and Wheeler 2002). There is some evidence of reduced daily average upwelling transport for 2015 and 2023, but less so for 2018 (Table 3). For years with negative El Niño-Southern Oscillation indices (2017, 2020, 2021, and 2022), enhanced upwelling is inferred, but we do not observe a simple relationship between El Niño-Southern Oscillation state and daily average upwelling transport magnitude. Coincidently, the cross-shelf differences in biomass isopleths show vastly larger offshore distances during those years (Table 4). The year 2019 also had reduced upwelling, but the effect of El Niño-Southern Oscillation may be muted. It is possible that the atmospheric and regional drivers of the 2019 MHW contributed to a reduction of upwelling.

The 2019 MHW was present over the entire Oregon shelf for most of the analysis period (Fig. 3). There are two key areas where upwelling appears to have created the previously mentioned buffering effect (Peterson et al. 2016; Varela et al. 2021). The first area is the inshore portion of the NH Line near CE01 (Fig. 5). The reduced number of MHW days inshore of CE02 suggests that intermittent upwelling weakly buffered the area, allowing biomass to move out over areas of the mid-shelf. Another strong potential influence is the shape of the shelf and disruption of the upwelling jet by Heceta Bank located just south of CE02, which retains waters inshore and provides conditions that allow phytoplankton to bloom (Barth et al. 2000; Kudela et al. 2008; Venegas et al. 2008). The second area is the region south of Cape Blanco, known to be influenced by persistent upwelling, which likely contributed to this area's greater offshore distribution of phytoplankton biomass compared to the rest of the coastline.

Regional-scale atmospheric forcings have previously explained the presence of the 2019 MHW in the greater Northeast Pacific, but local acute processes (Ekman transport) also influence the presence of MHW events over the Oregon shelf. As the Aleutian Low pressure system weakened, regional winds declined and shoaling of the surface mixed layer occurred along with reduced upwelling (Amaya et al. 2020). This likely allowed the MHW to propagate close to shore or persist at a location just offshore of the Oregon shelf. In this instance, the atmospheric forcings of the MHW (shifts and or weakening in pressure systems) are a significant contributor to the local MHW presence, although that is not explored in this work and may explain the few instances where MHW presence was observed despite indication of upwelling.

However, in instances where upwelling clearly acts as a buffer or shoreward barrier to MHWs, the opposite condition may also hold opposite consequences. This would then suggest that sustained periods of downwelling would draw portions or filaments of a MHW inshore. During discrete events, MHWs further inshore of CE04 initiated with downwelling and terminated with upwelling, suggesting that onshore Ekman transport captures MHW waters and brings them inshore (Supporting Information Figs. S1, S2). Marine heatwave waters are less dense than nearshore waters and displacement of phytoplankton biomass occurs further inshore in both contexts (Supporting Information Fig. S1,

S2). For shorter duration MHW events, wind and Ekman transport of less dense MHW waters contribute to the initial displacement of Chl *a*, while for longer MHW events, the prolonged presence of the regional MHW and its atmospheric drivers likely plays a more significant role. Marine heatwave presence at each site (Fig. 4; Supporting Information Figs. S1, S2) occasionally coincides with weak upwelling, suggesting the density gradient between MHW and upwelled masses also influences bloom compression.

Marine heatwaves identified at CE04 in 2018 are more readily explained by a warm freshwater lens originating from the Columbia River, which can extend hundreds of kilometers offshore and tens of meters deep (Saldías et al. 2016). The presence of the Columbia River Plume is most notable toward the beginning of each upwelling season with drastic dips in sea surface salinity down to 28–30 ASU at CE04 (Fig. 4) and CE02 (Supporting Information Fig. S1) but is less apparent later in the season. The plume has been observed at the mid-shelf off Newport, Oregon in the past, with indication that it slowly moves inshore over the course of the upwelling season (Mazzini et al. 2015). The salinities during the warm events in 2018, as well as select events in 2016 and 2022, are indicative of a warm freshwater plume from the Columbia River. In the case of the 2019 MHW, it was contemporary with reduced river discharge within the Columbia River Basin (Dodrill et al. 2023), suggesting this source of freshwater influence was minimal, making the observed density decrease primarily temperature driven. It is also apparent that sea water density associated with freshwater plumes is less than densities associated with MHWs by ~ 0.5 to 1 kg m^{-3}. A similar observation can be made for the salinity of each water mass, making it a useful tool for separating warm freshwater plumes from warm MHW waters.

Cervantes et al. (2024) compared in situ time series from CE02 and archived NH10 data to Optimum Interpolation SST V2 and found that the blended dataset typically overestimated daily mean SST during the summer months, which can lead to the potential for misidentification of MHWs and incorrect metrics. In review of MHWs not covered in great detail in prior literature (e.g., years not associated with the 2014–2015 and 2019 MHWs), it is important to keep this consideration in mind for both nearshore and offshore events. It is also important for readers to understand that modification of the suggested quantitative MHW definition, as we have done in this work, may result in different findings, particularly when it comes to establishing the timing and intensity of shorter events.

We recognize that the definitions of what constitutes a MHW may be problematic and variable depending on study purpose and goals (Amaya et al. 2023), particularly when considering the effects at finer spatial scales. We recommend that future analyses over the Oregon shelf use Blobtracker data or a globally gridded dataset as a first pass at identifying anomalously warm features in the greater Northeast Pacific and then perform methods described by Hobday et al. (2016, 2018) to identify and categorize anomalous warming further inshore on a finer spatial and temporal scales. This would aid in the determination of whether a nearshore MHW is derived from a parent MHW with a regional atmospheric driver, has more unique origins, or can be better explained by other physical phenomena.

Phytoplankton biomass and displacement during MHWs

Along the NH Line and near CE01 (~ 3 km offshore), we observed no substantial difference in Chl *a* concentrations between years (Fig. 6, CE01). The estimated distances given in Table 4 would imply that for 2015 and 2019, upwelling-driven biomass did not regularly reach as far offshore as other years and on average was confined somewhere between the OOI CE04 and CE02 sites. For short events, vertical transport direction and MHW status was variable, suggesting an even closer look at MHW density and bloom compression is needed. Averaged over a period of months; persistent, iterative, and intense MHWs like those associated with the 2019 MHW along with the upwelling influences from a regional atmospheric driver can result in the confinement of phytoplankton biomass upward of 9 km further inshore compared to periods not impacted by anomalous warming. Along the NH Line, this is roughly 25% of the shelf width (~ 40 km), suggesting that reduced upwelling and prolonged summertime MHWs compress blooms closer to shore, which could have cascading effects down to the seafloor on and off the shelf.

Future research

The interannual spatial differences in phytoplankton bloom extent, inferred here largely from patterns of Chl *a*, raises questions about the effects of MHWs on carbon export to benthic communities. Previously, Hales et al. (2006) described that alongshore transport and subsequent mineral ballasting, entrainment in the benthic boundary layer, and offshore benthic boundary layer transport may remove 65–92% of particulate organic carbon that is produced over the Oregon shelf. However, Reimers and Fogaren (2021) argue that high rates of benthic respiration during winter months require significant particulate organic carbon delivery to and retention by the seabed of this dynamic shelf. The compression of biomass further inshore and in a restricted surface mixed layer associated with chronic and intense MHWs may enhance shelf retention and reduce off-shelf export.

From fig. 10 of Evans et al. (2015), suppression or subduction of Chl *a* to depth can be observed in the cross-shelf. Anecdotally, surface temperatures approach a MHW classification during their analysis period in 2008. In CE02 profiler data for 2019, a similar subsurface Chl *a* signal can be observed, suggesting subduction of Chl *a* occurs at a MHW front. Further research is required to quantify the impacts of MHWs on carbon transported alongshore or carbon that is delivered to greater depths beyond the shelf break. Long-term

observational programs and new technologies will be key in these assessments. As a consequence of the spatial change in overlying phytoplankton biomass, there may also be ecological impacts on sessile and migratory communities that occur between the OOI CE04 and CE02 sites, particularly on those that line the shelf break.

Conclusion

Using open-access data, we documented a reduction in the average offshore distribution of summer upwelling-driven phytoplankton blooms off the Oregon coast during periods of significant anomalous warming. These warming events were associated with parent MHWs that occurred within the greater Northeast Pacific, whose primary atmospheric driver was also known to reduce surface winds and upwelling. The result is the presence of MHWs over the shelf and the compression of concentrated phytoplankton biomass at least 9 km further inshore compared to non-MHW periods along the NH Line during the upwelling season. The observed effect along the northern Oregon shelf is also a spatially restricted distribution of Chl *a* inshore of the shelf break during MHWs. During normal non-MHW conditions, biomass will extend out to the shelf break and beyond. The biophysical effects of MHWs on Chl *a* distribution along the southern coast is less significant and reduced biomass is more likely connected to differences in nutrient flux, transport, and the physiological impacts of MHWs. As MHWs are predicted to intensify and increase in frequency in the future, the biophysical influences of their drivers and anomalous temperatures on the spatial distribution of phytoplankton, in addition to the physiological effects, should be further examined when performing regional and local studies.

Data availability statement

We provide setup instructions, Jupyter Notebooks, and modules under an MIT License to facilitate replication of our analysis (https://github.com/IanTBlack/oregon-shelf-mhw). A list of the packages used in analysis and visualization can be found in the repository requirements.txt file. All data utilized in this project are from publicly accessible repositories (*see* project repository README for links). Processing and analysis were done in Python (≥ 3.10) on hardware provided through the OOI JupyterHub service (https://jupyter.oceanobservatories.org/).

References

Amaya, D. J., N. E. Bond, A. J. Miller, and M. J. DeFlorio. 2016. The evolution and known atmospheric forcing mechanisms behind the 2013–2015. North Pacific warm anomalies. US Clivar Variations **14**: 1–6. Availble from https://www.researchgate.net/publication/303720753_The_evolution_and_known_atmospheric_forcing_mechanisms_behind_the_2013-2015_North_Pacific_warm_anomalies

Amaya, D. J., A. J. Miller, S.-P. Xie, and Y. Kosaka. 2020. Physical drivers of the summer 2019 North Pacific marine heatwave. Nat. Commun. **11**: 1903. doi:10.1038/s41467-020-15820-w

Amaya, D. J., and others. 2023. Marine heatwaves need clear definitions so coastal communities can adapt. Nature **616**: 29–32. doi:10.1038/d41586-023-00924-2

Baker, K. G., and R. J. Geider. 2021. Phytoplankton mortality in a changing thermal seascape. Glob. Chang. Biol. **27**: 5253–5261. doi:10.1111/gcb.15772

Barna, A., E. Firing, and F. Fernandes. 2024. GSW-python (version 3.6.17.post1) [Computer software]. Available from https://pypi.org/project/gsw/

Barth, J. A., S. D. Pierce, and R. L. Smith. 2000. A separating coastal upwelling jet at Cape Blanco, Oregon and its connection to the California Current System. Deep-Sea Res. II Top. Stud. Oceanogr. **47**: 783–810. doi:10.1016/S0967-0645(99)00127-7

Barth, J. A., and others. 2019. Better regional ocean observing through cross-national cooperation: A case study from the Northeast Pacific. Front. Mar. Sci. **6**: 93. doi:10.3389/fmars.2019.00093

Batten, S. D., C. Ostle, P. Hélaouët, and A. W. Walne. 2022. Responses of Gulf of Alaska plankton communities to a marine heat wave. Deep-Sea Res. II Top. Stud. Oceanogr. **195**: 105002. doi:10.1016/j.dsr2.2021.105002

Behrenfeld, M. J., E. Boss, D. A. Siegel, and D. M. Shea. 2005. Carbon-based ocean productivity and phytoplankton physiology from space. Global Biogeochem. Cycles **19**: 2004GB002299. doi:10.1029/2004GB002299

Blondeau-Patissier, D., J. F. R. Gower, A. G. Dekker, S. R. Phinn, and V. E. Brando. 2014. A review of ocean color remote sensing methods and statistical techniques for the detection, mapping and analysis of phytoplankton blooms in coastal and open oceans. Prog. Oceanogr. **123**: 123–144. doi:10.1016/j.pocean.2013.12.008

Bond, N. A., M. F. Cronin, H. Freeland, and N. Mantua. 2015. Causes and impacts of the 2014 warm anomaly in the NE Pacific. Geophys. Res. Lett. **42**: 3414–3420. doi:10.1002/2015GL063306

Boyd, P. W., H. Claustre, M. Levy, D. A. Siegel, and T. Weber. 2019. Multi-faceted particle pumps drive carbon sequestration in the ocean. Nature **568**: 327–335. doi:10.1038/s41586-019-1098-2

Cervantes, B. T., M. R. Fewings, and C. M. Risien. 2024. Subsurface temperature anomalies off Central Oregon during 2014–2021. J. Geophys. Res. Oceans **129**: e2023JC020565. doi:10.1029/2023JC020565

Checkley, D. M., and J. A. Barth. 2009. Patterns and processes in the California Current System. Prog. Oceanogr. **83**: 49–64. doi:10.1016/j.pocean.2009.07.028

Corwith, H. L., and P. A. Wheeler. 2002. El Niño related variations in nutrient and chlorophyll distributions off Oregon. Prog. Oceanogr. **54**: 361–380. doi:10.1016/S0079-6611(02)00058-7

Dodrill, T. N., Y. Pan, and T. D. Peterson. 2023. River discharge mediates extent of phytoplankton and harmful algal bloom habitat in the Columbia River Estuary (USA) during North Pacific marine heat waves. Estuar. Coasts **46**: 166–181. doi:10.1007/s12237-022-01129-y

Dunne, J. P., J. L. Sarmiento, and A. Gnanadesikan. 2007. A synthesis of global particle export from the surface ocean and cycling through the ocean interior and on the seafloor: Global particle export and cycling. Global Biogeochem. Cycles **21**: GB4006. doi:10.1029/2006GB002907

Evans, W., B. Hales, P. G. Strutton, R. K. Shearman, and J. A. Barth. 2015. Failure to bloom: Intense upwelling results in negligible phytoplankton response and prolonged CO_2 outgassing over the Oregon shelf. J. Geophys. Res. Oceans **120**: 1446–1461. doi:10.1002/2014JC010580

Fewings, M. R., and K. S. Brown. 2019. Regional structure in the marine heat wave of summer 2015 off the Western United States. Front. Mar. Sci. **6**: 564. doi:10.3389/fmars.2019.00564

Frölicher, T. L., E. M. Fischer, and N. Gruber. 2018. Marine heatwaves under global warming. Nature **560**: 360–364. doi:10.1038/s41586-018-0383-9

Hales, B., L. Karp-Boss, A. Perlin, and P. A. Wheeler. 2006. Oxygen production and carbon sequestration in an upwelling coastal margin: Coastal margin production and sequestration. Global Biogeochem. Cycles **20**: GB3001. doi:10.1029/2005GB002517

Hayashida, H., R. J. Matear, and P. G. Strutton. 2020. Background nutrient concentration determines phytoplankton bloom response to marine heatwaves. Glob. Chang. Biol. **26**: 4800–4811. doi:10.1111/gcb.15255

Hobday, A., and others. 2016. A hierarchical approach to defining marine heatwaves. Prog. Oceanogr. **141**: 227–238. doi:10.1016/j.pocean.2015.12.014

Hobday, A., and others. 2018. Categorizing and naming marine heatwaves. Oceanography **31:**162-173 doi:10.5670/oceanog.2018.205

Holmes, C. V. 2007. Mean spring and fall upwelling transition dates off the Oregon and Washington coasts. Available at https://www.cbr.washington.edu/dart/trans

Huot, Y., M. Babin, F. Bruyant, C. Grob, M. S. Twardowski, and H. Claustre. 2007. Relationship between photosynthetic parameters and different proxies of phytoplankton biomass in the subtropical ocean. Biogeosciences **4**: 853–868. doi:10.5194/bg-4-853-2007

International Hydrographic Organization. 2024. GEBCO, 2023 [Dataset]. Available from https://www.gebco.net/data_and_products/gridded_bathymetry_data/

Jacox, M. 2024. Coastal Upwelling Transport Index [netCDF4]. Available from https://mjacox.com/upwelling-indices/

Jacox, M. G., C. A. Edwards, E. L. Hazen, and S. J. Bograd. 2018. Coastal upwelling revisited: Ekman, Bakun, and improved upwelling indices for the U.S. West Coast. J. Geophys. Res. Oceans **123**: 7332–7350. doi:10.1029/2018JC014187

Kämpf, J., and P. Chapman. 2016. Upwelling systems of the world. Springer International Publishing. doi:10.1007/978-3-319-42524-5

Kavanaugh, M., F. Abdala, H. Ducklow, D. Glover, W. Fraser, D. Martinson, S. Stammerjohn, O. Schofield, and S. Doney. 2015. Effect of continental shelf canyons on phytoplankton biomass and community composition along the western Antarctic Peninsula. Mar. Ecol. Prog. Ser. **524**: 11–26. doi:10.3354/meps11189

Kudela, R., N. Banas, J. Barth, E. Frame, D. Jay, J. Largier, E. Lessard, T. Peterson, and A. Vander Woude. 2008. New insights into the controls and mechanisms of plankton productivity in coastal upwelling waters of the Northern California Current system. Oceanography **21**: 46–59.

Leising, A., L. DeWitt, and G. Williams. 2024. The California Current marine heatwave tracker—blobtracker [Dataset]. Available from https://www.integratedecosystemassessment.noaa.gov/regions/california-current/california-current-marine-heatwave-tracker-blobtracker

Mazzini, P. L. F., and others. 2015. Anomalous near-surface low-salinity pulses off the Central Oregon coast. Sci. Rep. **5**: 17145. doi:10.1038/srep17145

NASA. 2022. NASA MODIS data product specifications. Available from https://modis.gsfc.nasa.gov/data/dataprod/

NOAA. 2023. OISSTv2 data product information [Dataset]. Available from https://www.ncei.noaa.gov/products/optimum-interpolation-sst

Noh, K. M., H.-G. Lim, and J.-S. Kug. 2022. Global chlorophyll responses to marine heatwaves in satellite ocean color. Environ. Res. Lett. **17**: 064034. doi:10.1088/1748-9326/ac70ec

Oliver, E. C. J., and others. 2018. Longer and more frequent marine heatwaves over the past century. Nat. Commun. **9**: 1324. doi:10.1038/s41467-018-03732-9

OOI. 2022. OOI observation and sampling approach. Available from https://oceanobservatories.org/wp-content/uploads/2022/08/1102-00200_Observation_and_Sampling_Approach_OOI_2022-01-26_Ver_1-09.pdf

OOI. 2023. OOI quality control. Available from https://oceanobservatories.org/quality-control/

Palevsky, H. I., Clayton, S., Atamanchuk, D., Battisti, R., Batryn, J., Bourbonnais, A., et al. 2023. OOI Biogeochemical Sensor Data: Best Practices & User Guide, Version 1.1.1. Ocean Observatories Initiative, Biogeochemical Sensor Data Working Group, 135 pp. Available from https://doi.org/10.25607/OBP-1865.2

Peterson, W., N. Bond, and M. Robert. 2016. The Blob (part three): Going, going, gone? PICES Press. North Pacific Marine Science Organization **24**: 46–48.

Reimers, C. E., and K. E. Fogaren. 2021. Bottom boundary layer oxygen fluxes during winter on the Oregon shelf. J. Geophys. Res. Oceans **126**: 2020JC016828. doi:10.1029/2020JC016828

Remy, M., H. Hillebrand, and S. Flöder. 2017. Stability of marine phytoplankton communities facing stress related to

global change: Interactive effects of heat waves and turbidity. J. Exp. Mar. Biol. Ecol. **497**: 219–229. doi:10.1016/j.jembe.2017.10.002

Risien, C. M., M. R. Fewings, J. L. Fisher, J. O. Peterson, and C. A. Morgan. 2022. Spatially gridded cross-shelf hydrographic sections and monthly climatologies from shipboard survey data collected along the Newport Hydrographic Line, 1997–2021. Data Brief **41**: 107922. doi:10.1016/j.dib.2022.107922

Risien, C. M., B. T. Cervantes, M. R. Fewings, J. A. Barth, and P. M. Kosro. 2023. A stitch in time: Combining more than two decades of mooring data from the central Oregon shelf. Data Brief **48**: 109041. doi:10.1016/j.dib.2023.109041

Saldías, G. S., R. Kipp Shearman, J. A. Barth, and N. Tufillaro. 2016. Optics of the offshore Columbia River plume from glider observations and satellite imagery. J. Geophys. Res. Oceans **121**: 2367–2384. doi:10.1002/2015JC011431

Sarmiento, J. L., and Gruber, N. (2006). Ocean biogeochemical dynamics. Princeton University Press.

Samuels, T., T. A. Rynearson, and S. Collins. 2021. Surviving heatwaves: Thermal experience predicts life and death in a Southern Ocean diatom. Front. Mar. Sci. **8**: 600343. doi:10.3389/fmars.2021.600343

Santora, J. A., and others. 2020. Habitat compression and ecosystem shifts as potential links between marine heatwave and record whale entanglements. Nat. Commun. **11**: 536. doi:10.1038/s41467-019-14215-w

Sen Gupta, A., and others. 2020. Drivers and impacts of the most extreme marine heatwave events. Sci. Rep. **10**: 19359. doi:10.1038/s41598-020-75445-3

Smale, D. A., and others. 2019. Marine heatwaves threaten global biodiversity and the provision of ecosystem services. Nat. Clim. Change **9**: 306–312. doi:10.1038/s41558-019-0412-1

Smith, K. E., M. T. Burrows, A. J. Hobday, N. G. King, P. J. Moore, A. Sen Gupta, M. S. Thomsen, T. Wernberg, and D. A. Smale. 2023. Biological impacts of marine heatwaves. Ann. Rev. Mar. Sci. **15**: 119–145. doi:10.1146/annurev-marine-032122-121437

Stukel, M., and others. 2017. Mesoscale ocean fronts enhance carbon export due to gravitational sinking and subduction. Proc. Natl. Acad. Sci. USA **114**: 1252–1257. doi:10.1073/pnas.1609435114

Stukel, M., H. Song, R. Goericke, and A. J. Miller. 2018. The role of subduction and gravitational sinking in particle export, carbon sequestration, and the remineralization length scale in the California Current Ecosystem. Limnol. Oceanogr. **63**: 363–383. doi:10.1002/lno.10636

Suryan, R., and others. 2021. Ecosystem response persists after a prolonged marine heatwave. Sci. Rep. **11**: 6235. doi:10.1038/s41598-021-83818-5

Tweddle, J., and others. 2010. Relationships among upwelling, phytoplankton blooms, and phycotoxins in coastal Oregon shellfish. Mar. Ecol. Prog. Ser. **405**: 131–145. doi:10.3354/meps08497

Varela, R., L. Rodríguez-Díaz, M. De Castro, and M. Gómez-Gesteira. 2021. Influence of Eastern Upwelling systems on marine heatwaves occurrence. Global Planet. Change **196**: 103379. doi:10.1016/j.gloplacha.2020.103379

Venegas, R. M., P. T. Strub, E. Beier, R. Letelier, A. C. Thomas, T. Cowles, C. James, L. Soto-Mardones, and C. Cabrera. 2008. Satellite-derived variability in chlorophyll, wind stress, sea surface height, and temperature in the northern California Current System. J. Geophys. Res. Oceans **113**: 2007JC004481. doi:10.1029/2007JC004481

Wyatt, A. M., L. Resplandy, and A. Marchetti. 2022. Ecosystem impacts of marine heat waves in the northeast Pacific. Biogeosciences **19**: 5689–5705. doi:10.5194/bg-19-5689-2022

Acknowledgments

Thank you to Melanie Fewings for providing feedback on the later stages of this manuscript. Thank you to Craig Risien for access to the OOI JupyterHub and its computing resources. The National Science Foundation provided salary support for IB and CER during the preparation of this work under award number OCE-1748726. CER was also supported by award number OCE-2126112. MTK was supported by the National Aeronautics and Space Administration Award Number 80NSSC20M0008.

Conflict of Interest

None declared.

Submitted 29 September 2023
Revised 26 April 2024
Accepted 16 November 2024

Associate editor: Yui Takeshita